Modular Smart Solid Wing-sail

Tyler Peterson, Eric Cao, Johnny McCullough
Jack Baskin School of Engineering
University of California, Santa Cruz
tepeters@ucsc.edu, ecao1@ucsc.edu, jmccullo@ucsc.edu

Gabriel Elkaim
Autonomous Systems Lab
University of California, Santa Cruz

Abstract— The purpose of this project is to prototype a modular autonomous solid wing-sail unit to be used as a primary and/or assistive propulsion system for seafaring vessels. The unit would act with fully autonomous response to its surrounding environment, continually generating the closest possible resemblance of a user's desired propulsion magnitude and direction. This unit would be put to immediate use in the re-envisioning of the Atlantis project, from which is the original concept genesis. But, beyond its initial intended use, a modular wind driven propulsion unit such as this would have a myriad of other applications ranging from trans-oceanic transit to small vessel recreational use. The Current progress of this project is documented here.

Keywords—Wing Sail, Autonomous Boat, Sailing, Controls

I. INTRODUCTION

A modular and robust wind-powered propulsion system capable of straightforward installation and autonomous operation on commercial or research vessels has found increasing interest and funding as fuel prices continue to increase and the need for autonomous sea-craft for remote oceanic sensing become more valuable. No wind-powered propulsion design has shown its ability to meet these needs more than the vertical winged propulsion system. This document will present the winged system and the evolution of the design over the years which will put into context the reasons for why this system has become a viable source of propulsion in the field of oceanic transport. The mechanics of the system and the necessary sensing devices to control the system will be analyzed so that the simplicity of the winged system can be better understood. Furthermore, to better appreciate the growing need for such a design, the numerous applications associated with winged sailing craft will be considered. This includes the use of relatively small winged vessels for unmanned oceanic research and exploration as well as the incorporation of large modular wing systems onto modern transport vessels to offset growing fuel costs. Finally the progress of the design and implementation of a prototype modular wing-sail will be discussed.

II. BACKGROUND

A. History

The concept of wing based propulsion systems arguably has been around since the first attempt at creating aircraft. Wind energy has been used for thousands of years to produce useful forms of power to propel sailing vessels for transportation. Although sailing transportation has been replaced by diesel powered propeller based vessels, the move to a hybrid system of combustion power and wind powered vessel propulsion has sparked great curiosity as large transport shipping vessels, that cater to over "90% of the world trade … carried by the international shipping industry" [2], would stand to save a considerable amount on fuel cost and reduce toxic combustion emissions. Therefore the design of a modular, robust, wind-powered system that could be installed on commercial vessels has found increasing support and funding, and no other design has seen more attention than the wing-sail.

To confidently design winged propulsion systems for sailing craft we must first understand the history behind the winged system and the evolution of the design over the years which puts into context the reasons why this system has become a viable source of propulsion in the field of oceanic transport. Many attempts have been made over the last 100 years to implement a wing propelled sailing craft, and in that time almost every possible configuration of the wing-sail has been tried.

The Flettner Rotor

Examining the success and failure of historical winged designs enables us to better understand what must be included and excluded in a successful design. The first documented mention of using a wing based propulsion system was in 1922 by Anton Flettner who added a cylindrical wing, later known as the Flettner Rotor, to a 200 foot vessel[1]. The Flettner Rotor showed great promise as a semi passive propulsion system that used the Magnus Effect to generate lift, but the continued funding for the design was cut short as Flettner's aeronautical designs were required in the war effort to advance helicopter research. The vessel and its relatively large wing-like devices can be seen in the image below along with an example of the spinning Flettner Rotor generating lift using the Magnus

Effect in a similar fashion to a solid wing, where a high pressure system is developed in the rear of the spinning cylinder and a low pressure system is generated in the front creating force perpendicular to the wind direction propelling the vessel forward.

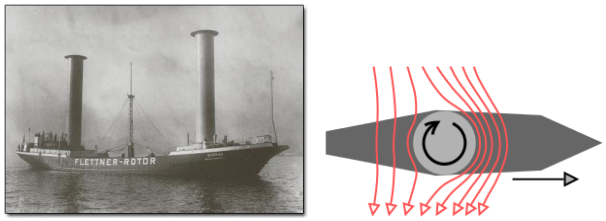

Figure 1: The Flettner Rotor mounted on a sailing vessel[3], The Magnus Effect on a Flettner Rotor[3]

However the mechanical nature of the Magnus Rotor adds complexity to the winged design that is not necessary for wind based propulsion. Furthermore the rotors are spun using large onboard motors which lowers the efficiency of the rotor system greatly when compared to a wing design. A solid Wing-sail is therefore a much more feasible approach to wind propulsion since it does not need to incorporate external actuation to produce propulsion.

The Wing-sail was not patented in the United States until 1951[1]. The patented design simply attempted to replace the cloth sail by using an aluminum wing that was controlled using ropes, winches, and pulleys similar to a typical sailing vessel. Since the wing was still trimmed using conventional ropes and winches the design was only taking minor advantages of the use of a Wing-sail, as we will see the beauty of the concept is that the wing system can be designed to self-trim, greatly reducing the attention needed to man the vessel. Despite this design never taking off it was noted that it was possible to sail this particular configuration much higher into the oncoming wind than with a conventional cloth sail, making transport up wind more efficient since a lesser number of tacks had to be used to complete the same trip.

The Walker Wing-sail

The next notable configuration of the Wing-sail did in fact take advantage of the simple self-trimming ability of the wing. The configuration was proposed and designed by John Walker, an English aerospace engineer, and used a series of four stacked vertical wings trimmed using a leading edge called a canard. The combination of the main wing and canard system is referred to as a "sailset" which allows the system to adjust automatically to maintain propulsion even during small wind direction variations, trimming the wing much better than a person may be capable of. The vessel and wing system along with the physics explaining the design can be seen below in Figure 2. By rotating the canard around its mounting axis the tail-wing provides a vertical rotational moment about the wing configuration opposing the moment created by the main-wings. This allowed for a very simplistic method of positioning the wing into an optimal heading, providing propulsion in the desired direction with very little attention required by the user.

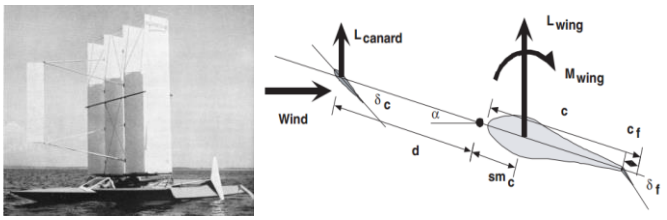

Figure 2: John Walkers Wing-sail boat [1], Wing-sail system analysis[1]

The free-body diagram above in Figure 2 describes the cross section of the wing and canard configuration as it appears in operation. The lift generated by the wing is accompanied by a moment created by the position of the wing from back to front in relation to the wind direction. This moment would cause the wing to rotate about its center and fall out of the optimal angle of attack to the oncoming wind. With the addition of the canard an opposing moment is created that resists the moment of the wing, balancing the moments allows us to easily set the optimal angle for the wing by adjusting the angle of the much smaller canard.

Walkers design was later refined and sailed across the Atlantic through hurricane conditions, proving the design was reliable and robust. Walker was noted for pushing the use of Wing-sails in commercial vessel applications, he was backed by Merchant Marine research that reported possible reductions in fuel cost between 34% and 50% [2]. Lack of correct marketing and production inefficiencies were blamed for the bankruptcy of the Walker Wing-sail Company.

The Atlantis

These designs all assisted and inspired the Atlantis project pursued by UCSC professor Gabriel Elkaim. The Atlantis project sought to create an autonomous wing-sailed Catamaran with the ability to efficiently complete unmanned routes in oceanic conditions using GPS and a litany of various sensors to overcome the various conditions along the way.

The Atlantis used a 17 foot tall by 5 foot wide Wing-sail to propel a 19 foot catamaran. The wing was suspended on a stub-mast and allowed to rotate freely about 360 degrees around the mast. The Wing-sail airfoil design was unique in respect to prior designs discussed earlier in that instead of the typical asymmetrical wing setup the Atlantis wing was made symmetric. Although an asymmetric wing has the ability to achieve better lift characteristics than a symmetric wing, a symmetric wing has the advantage of having identical characteristics in both directions of sail, greatly simplifying the characteristics of the propulsion and the required complexity of the control system. To increase the lift factor closer to that of an asymmetric wing an aileron was added

allowing for a dynamic adjustment of the wings airfoil shape and in turn its lift properties. A rendering of the Atlantis is seen below in Figure 3.

Figure 3: A rendering of the Atlantis project [1]

The Atlantis used a tail-wing to control the angle of attack of the main-wing. The tail-wing, as opposed to the canard described earlier, results in a system that tends to stability which lends itself much more to autonomous control.

The Atlantis was successful and shown to autonomously track a desired course to within 1 meter of the desired route. The Wing-sail design provided the Atlantis with an optimal wind propulsion method that was both more efficient than its cloth-sail predecessor and also much easier to control.

By examining the history behind the winged sail system and the evolution of the design over the years we can see that the most recent configurations of the design are far superior to any of its competitors in the area of wind propulsion. Furthermore the many applications of such a semi-passive wind propulsion system are yet to be discovered.

B. Applications

To better appreciate the growing need for an autonomous design the numerous applications associated with winged sailing craft will be considered. Although the applications of autonomous winged craft are numerous the various applications can be simplified into two categories that include the use of relatively small winged vessels for unmanned oceanic measurement and exploration, and the incorporation of large modular wing systems onto transport vessels to offset growing fuel costs.

Because the self-trimmed wing design simplifies the control of the system it becomes much easier to automate the wing and operate the vessels propulsion using an integration of GPS and environmental sensing. The automation of the wing allows the wing itself to be a modular part of the entire vessel only needing to receive the desired bearing that the vessel needs to travel in to create propulsion in that direction. The modularity of the design lends itself to being installed easily on small autonomous sailing crafts and installed in multiples on larger transport vessels. The following is a general and brief overview of these applications.

Ocean Monitoring

Autonomous sailing crafts are now being sought as platforms for low cost ocean research and monitoring. Current ocean monitoring is performed by manned survey vessels and by moored and drifting data buoys that relay measurements, via radio, to land stations. The presence of people in manned ocean surveys makes this method of ocean measurement prohibitively expensive leaving only the drifting or stationary buoy as a source of long term cost effective measurement. However drifting buoy stations are difficult to maintain contact with as they are subject to the movement of currents and changing weather patterns as well as having no ability to focus on an area of interest. In contrast moored buoys limit the measurements taken to a small oceanic location and require costly intervention to reposition. Remote monitoring systems like satellites and aircraft are also employed but it is generally agreed that ocean based systems produce measurements of greater meaning to researchers compared to these remote measurement systems.

It has been envisioned that great numbers of such vessels could be deployed to create an ocean sensing grid that could monitor vast areas with the ability to quickly reform their shape to focus on oceanic locations of interest [7]. Furthermore such a vessel has the potential to depart and return to a designated maintenance location for needed repairs as opposed to current moored and drifting designs that require manned vessels to find and extract them. Given the comparatively lower cost of an unmanned sailing vessel and the ability for such a vessel to move to precise locations they lend themselves to replace manned vessels, buoys, and remote monitoring of oceans.

Oil Spill Tracking

The mass transport of raw oil oversea as well as the increasing use of deep sea oil drilling to fulfill international energy needs has led to an increase in major ocean oil spills. Recovering the oil from an ocean spill is necessary to mitigate the long-term damage to the environment and to human life. Having real time data on the size of the oil slick generated by the spill, as well as the direction and speed at which it is drifting is essential to successful recovery operations. Currently the most feasible method of tracking a spill is using drifting buoys that can relay information about the spill to a central database. However the buoys are often separated from the oil slicks they have been deployed to track because of their different drift characteristics which make oil slicks much faster than the drifting buoys, and once separated, information can no longer be generated on the whereabouts of the slick. A more costly method of oil slick tracking employs the use of planes that fly above the drifting spills registering the slick with specialized radar detection. This method can only be used when weather and visibility permits but the increased dangers of night navigation over open ocean, the complications related to takeoff and landing in open ocean, as well as the limited endurance of aircraft due to the need to refuel, limits the viability of this form of tracking in most instances. The final

method often considered is satellite imaging to track the slick. This method however is rarely implemented due to the high costs and the inability for satellites to continue tracking the slick under cloud cover.

Considering the faults of these methods related to their cost and reliability it becomes clear that a design that uses a modular sail to generate directed propulsion to maintain contact with the oil slicks greatly improves on both the drifting buoy design as well as the aircraft and satellite imaging methods. A wind propelled vessel would have the ability to keep up with the oil slicks while also being unaffected by cloud cover and weather. Furthermore the cost of a wind propelled buoy is far less than satellite imaging or tracking by aircraft. The figure below illustrates a possible oil spill tracking system utilizing a network of autonomous sailing sensors measuring characteristics of a spill on multiple slick fronts. This information is relayed to large oil collecting vessels allowing for a more effective and efficient recovery operation.

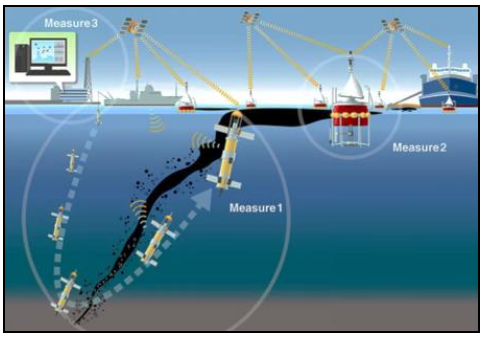

Figure 4: Rendering of autonomous oil spill tracking concept [6]

Although ideas like these might seem farfetched they comment on the ability of mass ocean presence by autonomous craft and their ability to collect data on our oceans and coastlines and create a low cost platform for other unmanned mobile ocean research projects.

Fuel Cost Reductions

Since the steady growth of globalization causing an increase in oceanic trade paralleled with rising fuel costs there has been continued interest among maritime researchers and trade and transport companies for developing a wind powered propulsion system for large commercial trading vessels. A large containership traveling at normal speed will burn 150 tons of fuel per day [8]. A study by a Dutch engineering firm confirmed that a containership fitted with numerous wings shown in 5 below had the potential to reduce fuel costs by 27%, saving 40 tons of fuel per day.

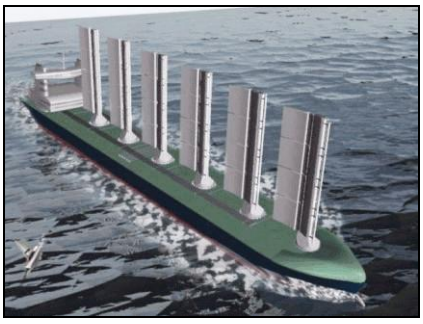

Figure 5: Rendering of a winged tanker concept [8]

Because ocean trade routes tend to follow the original routes developed when vessels were still only wind powered the routes often remain optimal for such a ship. Furthermore insurance associated with deep water towing due to engine failure have the potential to be eliminated as the ship would have the ability to sail into port at reduced speed. With fuel costs generally trending upward the design and retrofitting of cargo ships with wing-sail systems will become an emerging market.

III. METHODS

A. Research

1) Wing Dynamics

The three main reasons to use a wing-sail over a conventional cloth sail are efficiency of the propulsion generated, the lower actuation forces required to control the wing, and the simplicity of the control required for the wing-sail. The efficiency of a wing-sail over a conventional cloth sail can be seen in the coefficient of lift comparisons between the two. The coefficient of lift is a relation of the lift a body can generate with respect to the velocity and density of the fluid it moves through. For the wing-sail in question a coefficient of lift of up to 1.8 can be obtained and for a conventional cloth sail of comparable size a coefficient of 0.8 can be attained [1], making the wing-sail more than twice as aerodynamically efficient compared to the conventional cloth sail.

The actuation of the wing-sail requires much smaller actuators than a comparable cloth sail. Since conventional sails are controlled from the rear of a long boom with a center pressure combating the angle of the sail, a large force is necessary to maneuver the cloth sail. The wing-sail in comparison is balanced about its center and generates lift at the point in which it rotates as seen in the top-down cross section of the wing in Figure 6. Instead of moving the main-sail directly, as a conventional sail, the wing-sail is adjusted by actuating the much smaller tail wing. This tail wing requires much less force to actuate which saves both weight and cost of the propulsion system, thereby increasing the systems efficiency.

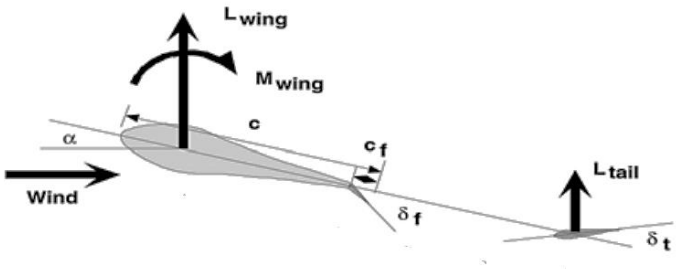

Figure 6: Cross section of the wing-sail and associated mechanics

The lift generated by the main wing is caused by the differential pressure system generated by the oncoming wind The pressure system is created by orienting the wing systems horizontal center line, termed the 'zero-lift line,' at an angle of attack relative to the wind direction. The angle of attack is shown as α in Figure 6. When α is zero, the wing generates no lift and slices through the air with minimal drag. When α is greater than zero, the wing directs a force or "lift" perpendicular to the wind direction, shown as Lwing. The intensity of lift is determined by wind intensity, air density, and an airfoil specific coefficient of lift, which is a function of α, the aspect ratio of the 3-d wing, and the wing's camber. The camber describes the ability of the airfoil to produce lift relative to drag. As α increases, the lift increases.

Drag is a force generated in the direction of the wind and is generally seen as detrimental to propulsion. In order to increase lift, reduce drag, and increase the camber of the wing, a flap is deployed. The flap causes a smoother flow of air around the wing and effectively increases the pressure gradient of the system without causing the corresponding drag to increase. The flap is shown as Cf at angle δf in Figure 6. A side effect of the flap is to produce a moment about the main wing's axis of rotation, which is shown as Mwing in Figure 6.

In order to control the angle of attack and counter act the moment produced by the flap, the tail wing is used. The tail wing is essentially a smaller version of the main wing and generates lift in the same manner. But since it is attached to the system at a distance('d' in Figure 6) from the main axis of rotation, the tail's lift creates a moment in the system. When the flap is not deployed, the main wing generates little to no moment about its axis of rotation and so the tail is oriented so it settles in the wind at a position where it generates no lift effectively setting α. When the flap is deployed, the tail angle is positioned to satisfy the desired angle of attack while also generating a moment to counter the flap.

The advantage to this wing a system is the simplicity of control. Since the wing-sail is self-trimming, meaning the angle of attack into the wind is made stable regardless of gusts or changing wind direction, the complexity of the control system is greatly reduced.

2) System Components

The system is mostly self-contained in that the controls,

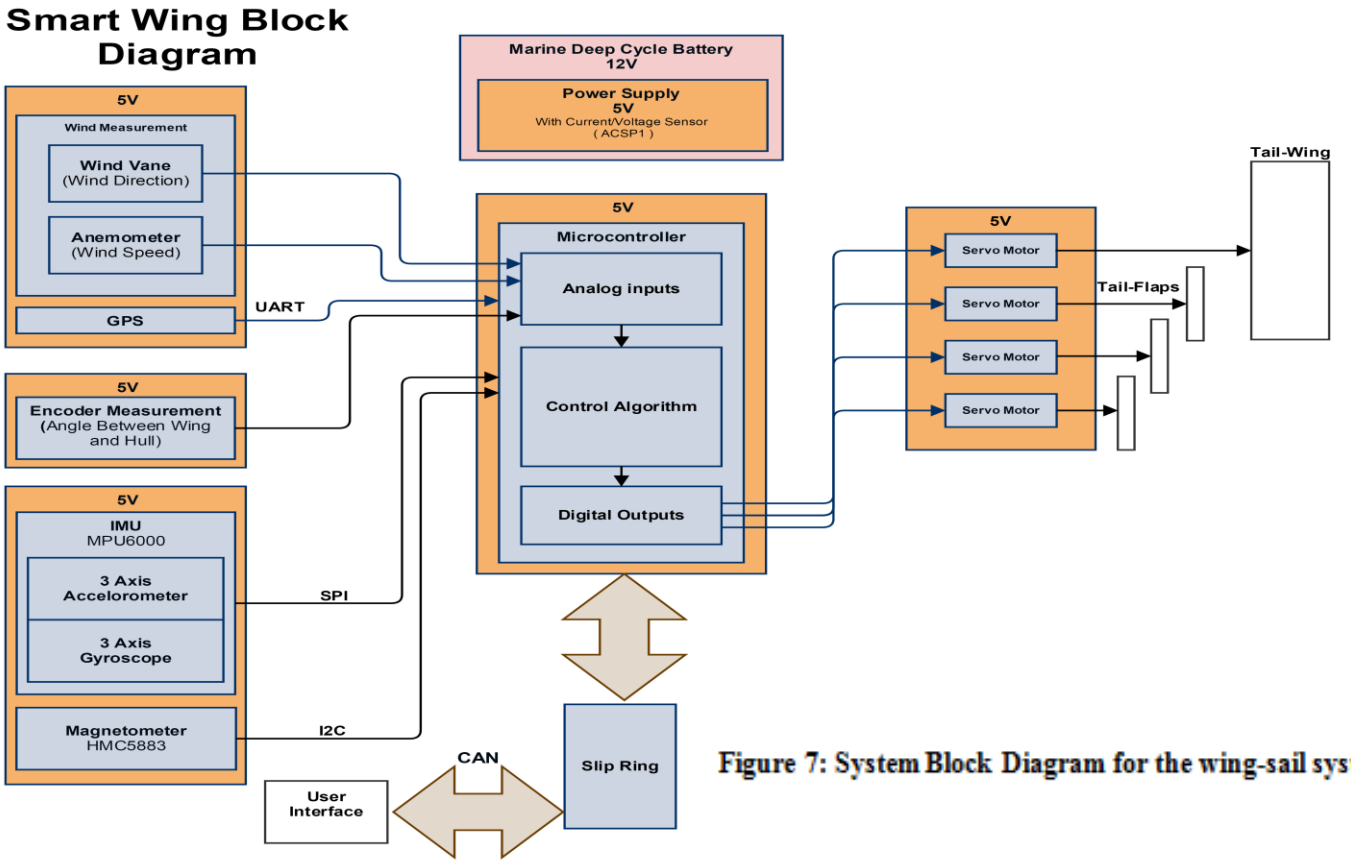

Figure 7: System Block Diagram for the wing-sail system

sensing, and actuation of the wing-sail are almost entirely done on the actual mechanical wing. The only information shared with the wing by the vessel is the hull direction that the intended propulsion will drive the vessel in as well as the percentage of maximum propulsion that the vessel needs to utilize. The wing-sail system will interpret the required vessel direction and percentage of maximum propulsion and then set the angle of the main-wing appropriately with respect to the angle of the incoming wind.

A block diagram of the intended wing-sail system design is found below in Figure 7. The diagram is intended to be read from left to right with the inputs to the system being fed into a microcontroller from the left and the output from the microcontroller used to drive the tail actuators labeled at the right.

Each block within the diagram above represents a critical module used to control the wing-sail. Wind measurements are taken using the anemometer and wind vane. The anemometer is used to measure the apparent wind speed and the direction of the wind is measured with the wind vane. The wing-sail's main-wing angle of attack can be modified by adjusting the angle of the tail-wing appropriately using these two measurements. The mechanics of this adjustment were examined in the wing dynamics section.
The Inertial Measurement Unit or IMU contains both an accelerometer and a gyroscope to measure the roll, pitch, and yaw of the vessel. The 3-axis gyroscope is used to measure the angle of the wing-sail relative to the horizon. By determining this angle the gyroscope measurement allows the system to detect if the vessel is capsizing and the wing can quickly adjust to correct the motion. This measurement is critical as the wing-sail has the potential to capsize the vessel it is installed on, and for an autonomous vessel this would be disastrous with no way to reorient. The 3-axis accelerometer measures the stability of the wing-vessel system. Small accelerations generated by vessel sway amongst waves must be accounted for before considering wind speed and wind direction measurements as a swaying vessel can generate perceived wind and wind direction that do not relate to the actual wind characteristics affecting the vessel.

The tail-wing actuator is used to adjust the angle of attack of the tail-wing which in turn will adjust the angle of attack of the main-wing. A potentiometer is used to measure the angle of the tail-wing with respect to the main wing and allows the tail-wing to be positioned precisely, generating the necessary angle quickly. The angle of the tail-wing and the relation to the main-wing's angle of attack is found below in Figure 6.
The slip ring allows for data transmission between the vessel and the wing-sail while still allowing the wing-sail to freely rotate about the mast. The system is powered using a rechargeable 12V deep cycle marine battery.

B. Design

1) Mechanical

Airfoil Section
The design of the main-wing and tail-wing was derived from Professor Gabriel Elkaim's aeronautical designs used in his Atlantis project. Attempting to design an airfoil section from the ground up was quickly regarded as impractical as no person on our design team has advanced knowledge of aeronautical physics or fluid dynamics. Instead, the airfoil section that was produced by Elkaim through design and simulation revisions was studied before it was implemented in our design so that we had a better understanding of the wing systems chosen aeronautical characteristics.

The first interesting choice for the design of the airfoil was the symmetry of the section. As asymmetrical airfoil sections can always achieve a greater lift coefficient it may seem that an asymmetrical section would be a better choice. However an asymmetric section will perform very differently depending on which point of sail our aquatic vessel is on. This alone allows us to realize that a symmetric wing makes for a much better design choice as it will produce identical lift coefficients in all mirrored points of sail reducing the complexity of the control system. The airfoil section design does however attempt pseudo asymmetry by using a tail-flap on the main wing that can be actuated to increase the coefficient of lift on all points of sail.

The second interesting design challenge was the need for the pitching moment of the main airfoil section to be small enough so that the main wing can easily be balanced by the tail wing as shown in Figure 6. By lowering the pitching moment the lift generated at the tail-wing, used to balance the main-wing's angle of attack, can be much smaller which allows the tail-wing's cord length and overall size to be much smaller. With a smaller tail-wing the moment of inertia of the entire wing system is decreased which in-turn decreases the wings response time adding to the system's ability to quickly respond to disturbances.

Using airfoil simulation software, Elkaim generated an airfoil cross section with the characteristics mentioned above, and provided us with an excel file that described the cross section mathematically as a function of the cross section's cord length. We produced a similar file in Solidworks that enabled us to scale the cross section to the appropriate size for our scaled down wing height.

The design of the tail section was identical to that of the main-wing except for the use of tail flaps. The ratio of main-wing area to tail-wing area was kept the same as described in Elkaim's thesis, as the needed lift to counter the main-wing pitching moment scales similarly.

The cross section was generated for our scaled cord length and the appropriate lightening holes and structural through holes were added to create what is referred to as the ribs of the wing.

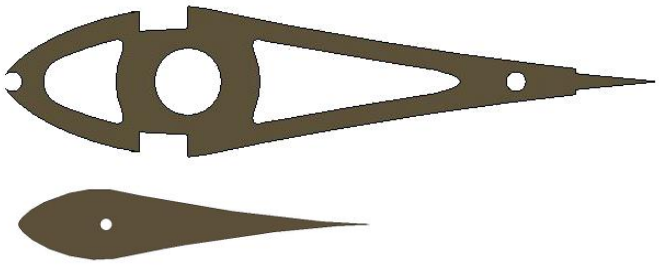

Figure 8: Main-wing and tail-wing rib developed from airfoil cross section calculations

The main-wing uses the rib shown above in Figure 8 as the cross section that defines the outline of the wing and was spaced uniformly from the bottom to the top of the main wing. The spacing of the ribs was also scaled to correspond to the original Atlantis design. Some ribs were designed with specialty purposes such as the servo rib that was not only produced to maintain the correct cross section though out the wing height but also to give us a mounting surface for the various actuators that control the angle of the tail-flaps and tail-wing. A rendering of the servo rib can be seen in Figure 9.

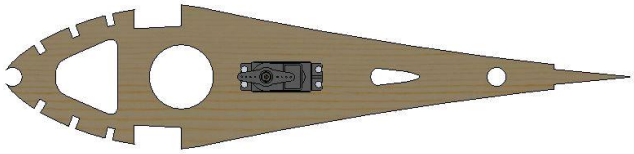

Figure 9: Rendering of main-wing servo rib

Since the ribs also require a vertical structure to enable their spacing and generate a vertical load bearing element of the wing, a series of vertical spacing elements were designed that fit in between each rib. These elements that run from the bottom to the top of the wing resemble spar elements that are typically found in airplane wings. A section of the spar can be seen in the Figure 10.

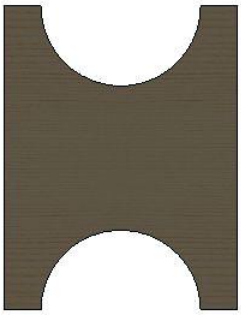

Figure 10: Rendering of typical spar element

The spar elements are paired with spar caps that are essentially long solid wood pieces running the length of the wing. Since the spars are bonded to the spar cap the design is better able to distribute vertical and bending loads throughout the main-wing frame and out to the ribs.

These two elements pieced together constitute a large portion of the main-wing frame. The full wing can be seen in the figure below. The addition of nose stringers that run up the front of the wing along with two tail slats that support the rear enable the structure to resist diagonal collapse of the structure that one might imagine would force the rectangular shape into more of a trapezoidal shape.

Since the bending load that the main-wing experiences is transferred through the spar and spar-cap the wing-sail, unlike a conventional sail, does not require a mast that runs the length of the sail. So instead of a full length mast a stub-mast was designed to couple the boat hull to the main wing. The stub-mast was designed to be secured to the hull of the boat while the wing-sail sits atop of it and left to spin freely. The free rotation of the main-wing is facilitated by the placing of a thrust bearing at the top of the stub-mast that interfaces to a bearing race mounted to a rib of the main wing. Similarly a needle bearing mounted to a lower rib resists the side loading of the main-wing.

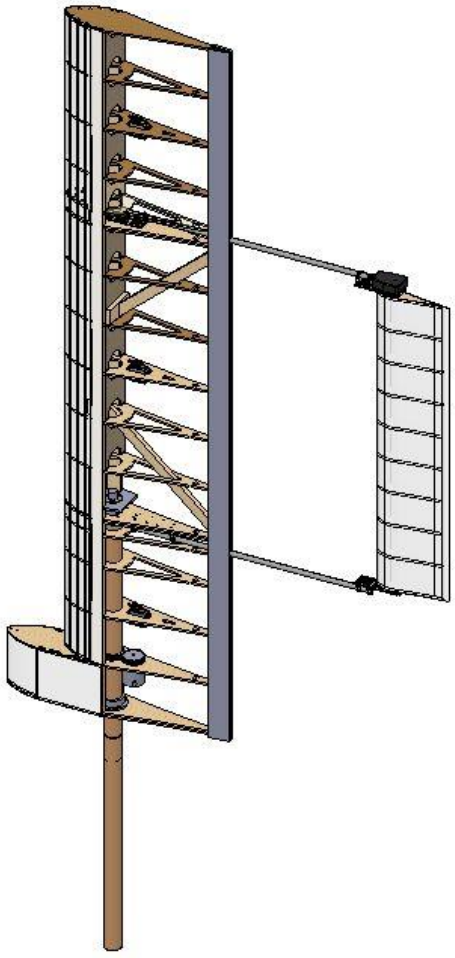

Figure 11: Rendering of complete wing

The tail-wing, unlike the main-wing, was designed to have a solid foam core, so as to remain light and maintain a lower inertial moment of the total wing, corresponding to a faster response time.

The tail-wing was designed to rotate between two mounts that are affixed to the main-wing via aluminum tubes. This structure comprises a frame that allows the main-wing to be actuated by the moment generated by the lift of the tail-wing. The tubing was chosen to be aluminum for its weight, stiffness and cost. A more costly but stronger and stiffer solution would be to use carbon fiber tubing for the frame. The frame is secured to the main-wing with mounts bolted to respective ribs. To support the extra weight of the tail-wing and frame, a 45^0 bracing was designed to run from the spars to the tails of the frame supporting ribs, preventing sagging of the rib tails and frame tubing due to the weight of the tail wing.

Because the Smart Wing system requires signals and power to be transferred from wing to vessel a slip ring mechanism was added to the design. The slip ring permits up to 12 signals or separate power lines to run from the vessel to the wing while still allowing the wing to rotate freely about the stub mast. A figure depicting the coupling of the slip ring, main-wing, and stub-mast, can be seen in Figure 12.

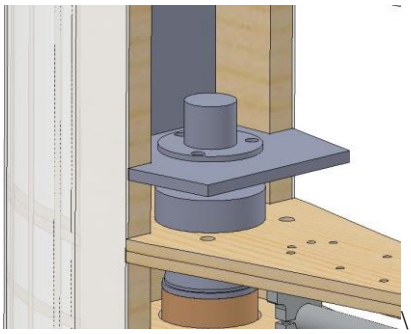

Figure 12: Slip ring from main wing to stub-mast

Finally the need to measure an absolute angular position of the main-wing to hull angle required the design of a rotational hull effect position sensor that is coupled to the stationary stub-mast via a one to one gearing. The gears were designed with a relatively small gear tooth to improve the surface area contact between the two gears. The gears can be seen in Figure 13.

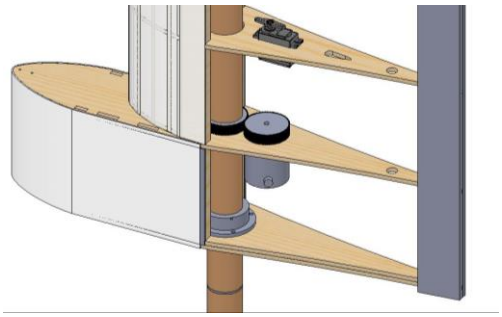

Figure 13: One to one gearing ratio for hull effect rotational sensor

2) Electrical

Actuators

The actuators for the wingsail were chosen based on several requirements. It needs to be reliable, as energy efficient as possible to decrease battery consumption, and powerful enough to overcome wind resistance when moving the control surfaces. The selection of the actuators involved a choice between DC motors or RC servos, as well as the method of actuation associated with each. A comparison between the two actuators and their actuation methods was made. Our options include using screw thread and lead screw to create a linear actuator with a DC motor, or use a RC servo with push-pull control rods to actuate the flaps and tail wing.

The DC motor linear actuator has the advantage of higher torque and the lead screw provides resistance to back-driving; which allows the motor to draw no current until the actuator's position needs to be changed. Its disadvantages include having a significantly higher stall current and increased mechanical complexity. The screw thread and lead screw might lead to binding due to unevenly distributed pressure or low tolerances in installation, making the actuation system less robust. The DC motor also requires a separate motor driver and additional feedback control system.

Figure 14: A DC motor with a lead screw

The RC servo with control rods introduces less mechanical complexity and consequently is more robust. It also draws less stall current than the DC motor and comes in a smaller form factor. All servos come in an integrated package with a motor driver and positional feedback controls, further reducing the complexity of the system. Some disadvantages of an RC servo include being susceptible to back driving from the control surfaces and being significantly more expensive to get torque comparable to a DC motor. It also has a quiescent current draw since it can't be turned off when stationary, unlike the DC motor linear actuator.

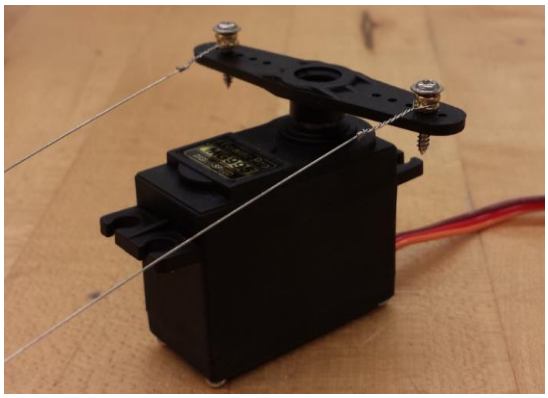

Figure 15: RC servo with control cables

After evaluating both systems, the RC servo with control rods was chosen to actuate the wing. The control rods were replaced with steel cables for flexibility and easier routing in our physical design.

Sensors

An encoder was needed to determine the position of the wing relative to the hull of the boat. The biggest issue encountered when choosing an encoder was finding one with an output format that would be easily read by our microcontroller. The absolute encoders we first looked at had the precision we required but most had grey code as the output where each individual bit had its own wire, and therefore required up to 8 I/O pins on the microcontroller to use. The ideal input format for the microcontroller would be an analog voltage value due to its simplicity and since there were several A/D pins available.

Figure 16: Absolute encoder with grey code output wires

The choice of requiring an analog output led to researching rotary potentiometers and Hall effect sensors (Figure 17) to create a variable voltage that is proportional to the wing to hull angle. After testing both, the Hall effect sensor was chosen to be the encoder due to it being more precise and not having a deadband, unlike the potentiometer. Another reason was because the Hall effect sensor has an internal voltage divider as a self contained package that outputs a voltage from 0 to 100% of your input voltage, as opposed to the potentiometer where we would have to build an external divider.

Figure 17: Hall effect sensor

Two of the most important sensors required on the wingsail are the wind speed and wind direction sensors. The two types of sensors are closely related, and are often integrated and sold as one unit which measures both. The biggest project requirements for this sensor were price and precision, along with its output type. Looking at potential wind sensors involved looking for compromises between all three categories. The main issue for our project was that the commercial sensors within our price range did not fit the other two requirements of precision and output format. Other sensors had the precision and output format we needed, but were priced way above our budget. Based on the three requirements mentioned, the Young 05305 wind sensor we received from Professor Mantey was almost ideal.

Figure 18: The Young 05305 wind sensor

The Young 05305 (Figure 18) wind speed and direction sensor was provided free of charge from the engineering department, which easily satisfies the project requirements regarding price. According to the data sheet, the wind speed sensor on the unit is capable of 0.9 mph resolution in wind speeds of up to 112 mph, and the wind direction sensor has a resolution of 5 degrees or below. These specifications are better than any other sensors within our budget and are more than precise enough for our purposes. The only part where it does not completely fit into our requirements is that one of the two sensor outputs is not something that can be read directly by the microcontroller. The wind position sensor is essentially a potentiometer with an internal voltage divider, and can be used directly by the microcontroller in the same way as the encoder mentioned earlier. The wind speed sensor output is an AC sine wave with varying amplitude and frequency proportional to the wind speed, which will require signal conditioning before being passed into the microcontroller.

Signal Conditioning

The goal of the signal conditioning circuit was to convert the AC sine wave coming from the wind speed sensor into something that is usable by the microcontroller. The best option would be to convert the AC signal into a DC voltage which can be fed into the ADC. The options were to convert the amplitude by rectifying the sinusoidal signal and using either a low pass filter or envelope detector to convert the amplitude into a DC voltage, or to take the zero crossings and convert the frequency information into a proportional DC voltage.

One possible method considered for converting the anemometer output into a signal that could be easily measured with our micro-controller was to use a zero crossing circuit. Since the output of the anemometer is a sine wave with varying amplitude and frequency as a function of wind speed, it was decided that isolating either the amplitude or frequency would allow us to more easily condition the measurement for interpretation in our microcontroller.

Using the zero crossing would allow us to set up an external interrupt that could measure the time between subsequent zero crossings, and since the time between zero crossings corresponds to the period of the anemometer frequency we would be able to calculate the wind speed.

When designing the zero crossing circuit a comparator was used to reference when the anemometer output crossed its reference voltage. However, since the anemometer output is an AC signal that is produced simply from an AC generator the zero crossing happens exactly at its reference which in our case will be the systems common ground. This means however that the comparator will have to be registering a zero crossing right at its rail, which makes for a less than ideal measurement. To remedy this, the anemometer signal was first sent through a summing amplifier that offset the zero crossing by 2.5 volts, halfway between our system voltage, and far from the comparators rails. The offset signal was then passed through an active filter with a 200 Hz cutoff frequency to roll off any noise that might cause errant switching of the comparator. The combined circuit can be seen in Figure 19.

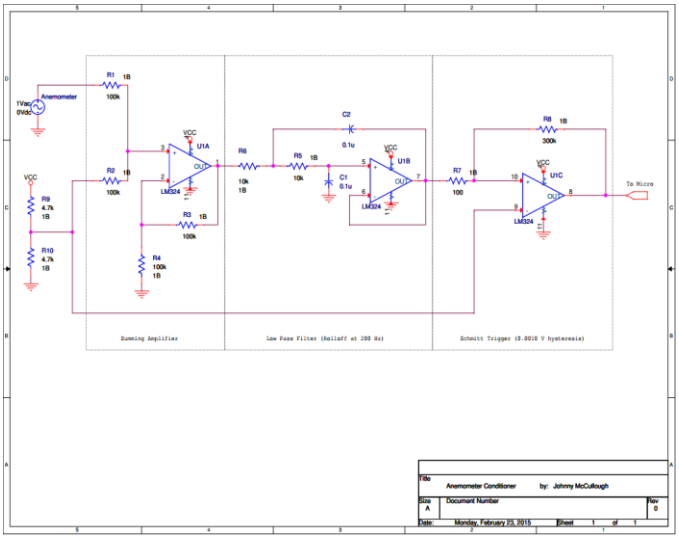

Figure 19: Zero Crossing Circuit

The comparator requires hysteresis in order to avoid switching due to noise around the zero crossing that our program would interpret as a false increased frequency and increased wind speed. A simulation of adequate hysteresis and inadequate hysteresis was performed and can be found Figure 20.

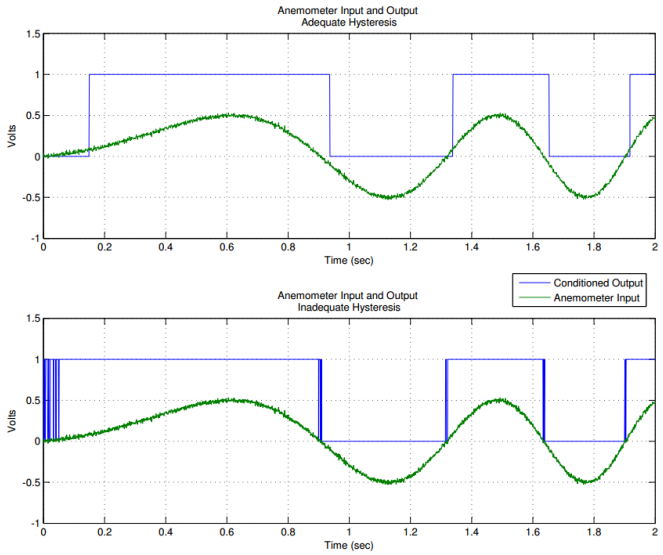

Figure 20: Adequate and Inadequate Hysteresis

It can be seen that if the hysteresis is designed to be relatively small we will risk the possibility of having errant switching and false wind speed measurements. However if the hysteresis were made to be arbitrarily large the circuit would fail to register zero crossings at lower wind speeds as they fail to produce a signal amplitude that is large enough to rise above

the hysteresis band. Through simulation and then experimentation with the actual circuit, a hysteresis of 1.0mV was found to produce the most useful measurement.

We decided to go with the frequency to voltage convertor since the data sheet for the wind sensor gives an equation relating the frequency of the signal to the wind speed, but gives nothing for the amplitude. If we were to use amplitude detection, we would have to experimentally plot and map out an equation relating the amplitude of the output signal and the wind speed, which is difficult since we do not have a way of generating a known speed or a sensor to measure it as we test using winds outside. The frequency information is also less susceptible to noise compared to using the amplitude of the signal.

The basic operation behind a frequency to voltage convertor consists of a comparator and a charge accumulator. The charge accumulator stores charge at a constant rate until the comparator detects the voltage has fallen below a certain threshold and triggers the accumulator. The accumulator then discharges through a resistor, creating a voltage. The measured voltage depends on the amount of current discharged through the resistor, which is proportional to the frequency at which the voltage drops and triggers the comparator.

Power Supply

As seen in the power budget in Figure 21, the stall current for the 4 servos makes up the majority of the power consumed, with the power being used by electronics and sensors almost negligible. The total max current that will be going through the 5V rail is around 8.4A, so we need to use a power supply rated for at least that amount.

	Component	Quantity	Current (mA)	Voltage (V)		Watts	5V Current (A)
1	MCU	1	105	3.3		0.3465	8.38054
2	Flash	1	40	3.3		0.132	
3	IMU	1	3.9	3.3		0.01287	
4	Compass	1	0.64	3.3		0.002112	
5	Pressure sensor	1	1	3.3		0.0033	
6	CAN bus	1	70	3.3		0.231	
7	FVC circuit	1	40	5		0.2	
8	Wind direction sensor	1	50	5		0.25	
9	Hall effect sensor	1	70	5		0.35	
10	RC servo	4	2000	5		40	
					Total (W)	41.52778	

Figure 21: The Power Budget

The total wattage for the power budget is around 42W. Dividing that by the 12V battery we plan to use, we get a current draw of 3.5A per hour. Using a battery life calculator, a 12V deep cycle battery rated at 90AH (amp hours) is required for a run time of 12 hours. This is for the maximum current draw at full stall current on every actuator, which is unlikely to happen often, so our informal estimation of the battery life for a 90AH battery is at least twice the calculated amount.

3) Controls

The overarching concept of the control of this system is to take in the current wind direction and compute an angle of the tail wing to produce a max possible thrust. Then, based upon physical and user defined parameters, the max thrust is limited. The modularity of this system is based in the ability to internally decipher the physics of the wing system and set a tail wing position in response to a user request. This modularity leads to the heart of the automated control aspect for this project.

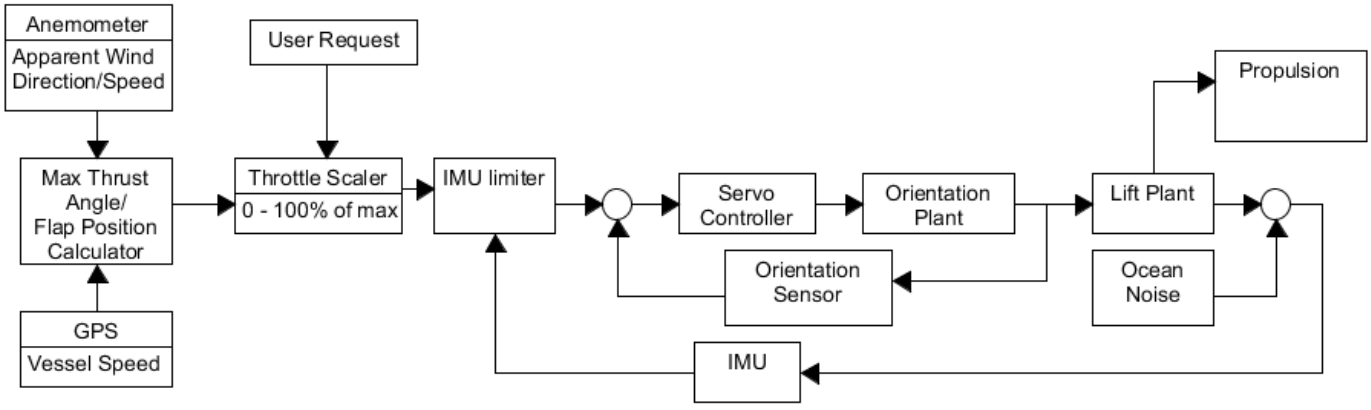

Figure 22: Concept Controller Diagram

In order to design our controller, two main aspects had to be identified. The first aspect is that the current state of our system is measured by our sensor array. The wing state consists of the current wing orientation with respect to the hull, the measured wind direction and intensity, vessel attitude, and the current hull speed. The second aspect is that we must define the natural response, or 'plant', of our system, which is outlined by the wing dynamics previously described. Bringing together the wing physics and state measurements, we created a conceptual design of our controller which is pictured in figure X.

Our concept controller works by first measuring the apparent wind direction/intensity from the anemometer and vessel speed from GPS and then computing the correlated flap and tail wing positions for max possible thrust. These max lift orientations are then scaled from 0 to 100 percent by the user input. The output from the desired throttle is then passed through another limiter, which has an effect determined by feedback from the IMU. The output from this limiter is fed into innermost feedback control loop. This loop drives the servos towards positions expected to cause the wing to orient to the desired angle. The actual output orientation is measured by the orientation encoder, which in turn feeds back to the servo control, causing adjustments to correct for error. This feedback loop is the heart of our controller.

The output from the main loop effectively goes through another plant, transforming itself to output lift. The combination of lift generated and noise in the form of ocean waves will affect the vessel attitude. The vessel attitude is measured via the IMU and subsequently the measurement is fed back to the earlier mentioned IMU driven limiter. This outer loop is applied for the purpose of preventing the vessel from capsizing if the lift generated is too extreme for the current environmental conditions.

C. Build

1) Mechanical

The mechanical nature of the Smart Wing and its organic shapes required a great deal of construction that ranged from fine carpentry to mill and lathe work, and even the use of composites to realize the Smart Wing's full form.

A great deal of the structure was created from wood, as it met the requirements for its light weight, ease of forming, strength, and cost. The Wing's ribs were constructed using a 0.25" thick cedar plywood. Using the airfoil sections created in Solidworks, we were able to cut out accurate airfoil sections quickly with the laser cutter. The plywood proved easy to cut with the laser and the resulting airfoil sections created were found to be sufficiently robust to continue with construction. The laser cutter can be seen in action in Figure 23 cutting various ribs.

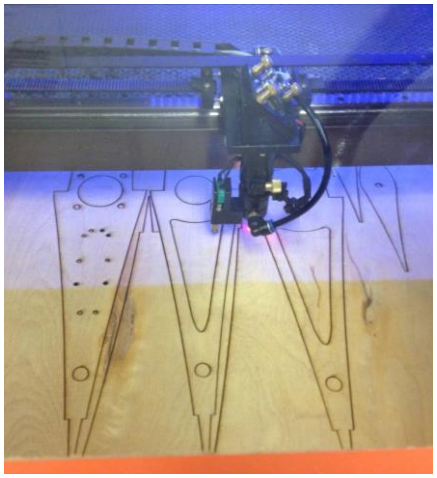

Figure 23: Laser Cutting the Ribs

Once the ribs were cut they were bonded to the spar and spar caps through a long and methodical process that restricted us to bonding one rib at a time and lots of waiting for the glue to set up. The work bench was used as a level surface that allowed all of the ribs to be set coincident to one another. Tyler Peterson can be seen applying his years of fine carpentry experience in Figure 24.

Once the main-wing skeleton was complete stringers were added to the nose to reinforce the surface that will experience a great deal of force. The skeleton can be seen in Figure 25.

Figure 24: Bonding the ribs to the spar caps

Figure 25: The main-wing skeleton

We next began construction on the tail-wing. It was decided to go with a composite shell over a Styrofoam core, as this would give us a tail-wing structure that is light, robust, and relatively cheap. To produce a Styrofoam core in the shape of our airfoil section a hotwire was constructed that allowed us to use the airfoil sections as guides for cutting the correct shape. This method, which is used in industry for many small winged personal aircraft, was found to be very effective. The hotwire process can be seen in the Figure 26.

Figure 26: Hotwiring the Styrofoam-core tail-wing

The final core resembled perfectly the required shape and was ready to receive its composite shell. The core can be seen in Figure 27.

Figure 27: Styrofoam tail-wing core

Aluminum tubes of 0.25" diameter were installed through the Styrofoam core to improve stiffness and enable attachment of a control horn to actuate the tail wing. Marine grade UV resistant epoxy and fiberglass was then applied in two layers to the Styrofoam core and allowed to cure to a stiff tough finish. The final tail-wing can be seen curing in Figure 28.

Figure 28: Tail-wing with fresh epoxy coat ready to cure overnight

The main-wing and tail-wing were then integrated producing our final structure as seen in Figure 29, standing vertically and free to rotate about the stub-mast. The Baskin School of

engineering logo was added to the wing in support of our fine establishment.

Figure 29: Total Smart Wing structure

2) Electrical

Actuators

The servos we bought initially were the Towerpro MG995, which were chosen based on their torque specifications and their price. They can output up to 11kg/cm of torque, which is more than enough to actuate the control surfaces we plan to use. However, upon receiving the servos, it was discovered that they had bad positional feedback and had problems centering precisely, which was not mentioned in the specifications.

Our solution to that involved ordering two upgraded versions of the servos to test as potential replacements. One is the MG996, which has the same specifications as the MG995 but with an upgraded PCB and IC control system to make it more accurate. The other is a HobbyKing MI servo with a magnetic induction sensor instead of a normal potentiometer for even more accurate control. During testing, both replacement servos were found to be much more accurate than the MG995. The three servos are picture in Figure 30.

For now, we have the MG995 servos installed onto the wingsail for testing and developing the feedback controls. Since the upgraded servos are the same size, they can be drop in replacements for the MG995.

Sensors

The Hall effect encoder arrived and was tested on a breadboard circuit to work as expected. We had planned to integrate it into the wingsail mast early on, but the dimensions of the one to one gearing for the mast and sensor turned out to be too small, and the first 3D printed versions of the gears did not fit onto their respective shafts. (Figure 31) The height of the teeth was also an issue, since they were too short and experienced slippage at certain points in the rotation of the mast. Because of these problems, we were unable to integrate the sensor onto the sail yet, since we are waiting on the 3D printing of the modified gears.

Figure 30: The 3 servos tested (From Left: HobbyKing MI, MG996, MG995)

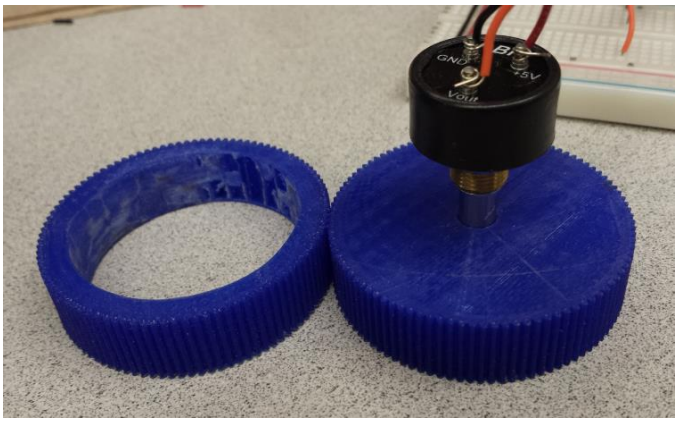

Figure 31: The Hall effect sensor and printed gears

The Young 05305 wind sensor we received was tested using the oscilloscope and found to be working as expected. The scope trace from the wind speed sensor portion was shown to be a sinusoidal signal which increased in both amplitude and frequency as the speed of the propeller is increased. The wind direction sensor worked similarly to the Hall effect sensor, in that a full revolution will swing the voltage from 0 to 100% of the input voltage and jump back again once the deadband is crossed. Once the sensor's functionality was verified, it was quickly integrated with both the power supply and signal conditioning circuit as soon as it was completed.

Signal Conditioning

Our design for the frequency to voltage converter is based on the LM331 Precision Voltage to Frequency Converter chip by Texas Instruments. The frequency to voltage configuration is given below, and can be adjusted to work with a 5V power supply. The circuit's frequency versus voltage output is specified to be linear within +/- 0.06% up to 10 kHz, which is more than enough considering that the highest wind speeds we expect to encounter would only result in a maximum frequency of roughly 200 Hz.

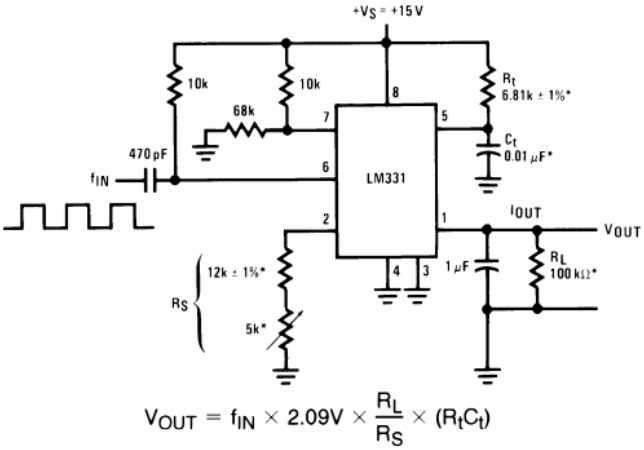

Figure 32: The LM331 Frequency to Voltage Circuit

After building the circuit as shown in Figure 32, there was still no output from it even after amplifying the AC sine signal from the wind speed sensor. After a long time trying to troubleshoot it, we realized that the circuit required a square wave input signal with a high rise time, which wasn't explicitly stated anywhere in the datasheet.

To overcome the problem, we had to add a circuit which converts the amplified sine wave into a square wave. A zero crossing detector circuit and a non-inverting Schmitt trigger were considered, and both were built and tested with the FVC.

Upon testing, the non-inverting Schmitt trigger induced a larger output in the frequency to voltage converter than the zero crossing detector, indicating it was more sensitive. Given that the Schmitt trigger was also simpler to build with 1 op amp versus 3, we decided to use the non-inverting Schmitt trigger in the frequency to voltage converter circuit.

After the Schmitt trigger and FVC were selected, a non-inverting amplifier stage was added both before and after the two circuits to boost input and output. The total number of op amps in this circuit is 3, so a MCP6004 quad op amp chip was used in the circuit. A low pass filter was added before the sine wave input from the sensor to filter out transient noise which caused errors in our Schmitt trigger output and another LPF was added before the output of the entire circuit was fed into the microcontroller's ADC, to smooth out ripples in the output voltage. After this was done the entire signal conditioning circuit was complete. The block diagram of the signal conditioning circuit is shown in Figure 33 and its wiring diagram is shown in Figure 34. Figure 35 Depicts the test circuit.

Power Supply

For power regulation we bought a 5V, 9A step down power regulator from Pololu called the D24V90F5(Figure 36). It has 80-95% efficiency and tested to have a ripple voltage of <1 mV, which was eliminated with a 3300 uF bypass capacitor

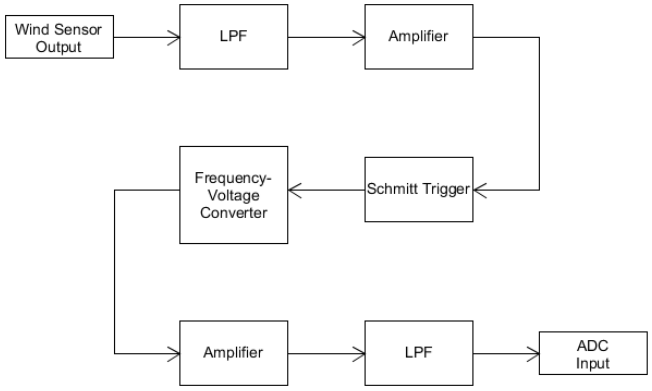

Figure 33: Signal conditioning block diagram

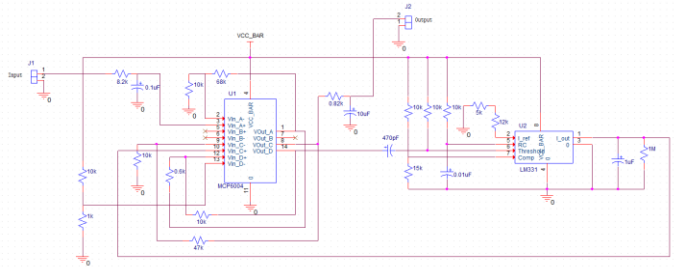

Figure 34: Signal conditioning wiring diagram

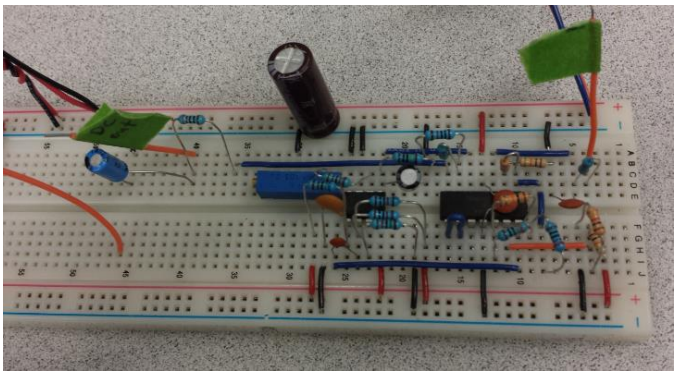

Figure 35: Signal conditioning breadboard circuit

.

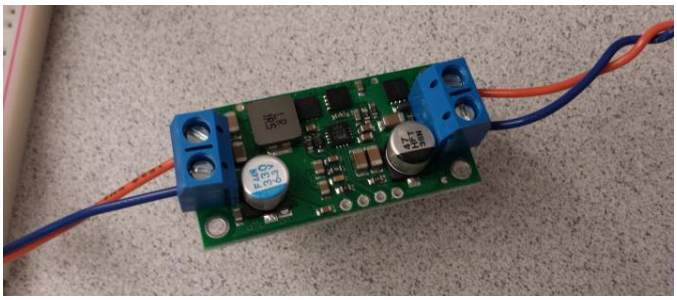

Figure 36: The D24V90F5 regulator

After verifying the functionality of our 5V regulator, it was integrated with all the circuits, sensors, and actuators mentioned previously to form our complete functional

electrical system. Figure 37 shows the components of the integrated system.

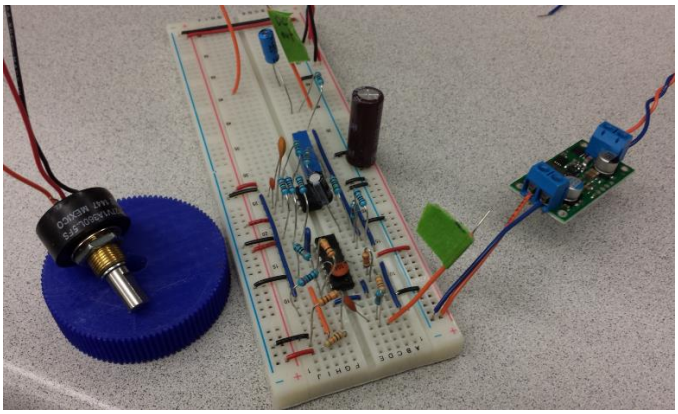

Figure 37: Several parts of the integrated system

3) Programming

The programming portion of the project is separated into two main sections, library modules and system controller.

I. Library Modules

The library modules are a controller clock set module, an ADC read module, a UART communication module, a servo control module, a CAN communication module, and an IMU read module.

Clock Set Module
The clock set module is used to configure our systems instruction rate. The module configures the PIC33 to use the AUAV3's provided external 8 MHz oscillator crystal, up scaled through an onboard phase locked loop capability, for setting the system MIPS. The module was written to allow the system MIPS to be set to 16, 32, or 64. These configurations give us a wide range of processor speeds while allowing correlated system adjustments to be done with simple powers of 2 factors. If necessary for the controller, the system MIPS can be increased up to 256 MIPS.

ADC Read Module
The ADC read module is used for reading the anemometer data, measuring current power supply voltage, measuring system current, measuring digital input reference voltage, and reading wing orientation encoder voltage. The ADC module is designed using the Pic33's 12 bit ADC and DMA peripheral read capabilities. When engaged, the ADCs are set to a continuous read mode at a rate of 3.3 KHz. The DMA operates in PING-PONG mode, constantly transferring each ADC port's unsigned 16 bit integer value to corresponding 128 word rolling buffers and a rolling sum. Each buffer is averaged using an 8 step bit shift to determine the ADC value, creating a fast moving average filter. The module configuration combined with AUAV3 onboard low pass filtering gives an extremely accurate ADC read with virtually no noise above the level of the 16 mV quantization error.

UART Communication Module
The UART communication module is currently configured to be used for serial communication with the controller for debugging and testing purposes. The serial takes advantage of two 512 byte rolling buffers with tail, head and current pointers. One buffer is used for transfer and the other for reception. Functions for printing strings and converting input strings to decimal values are used for interacting with and commanding the controller. In future, this module will also be used to read data from an external GPS, for the purpose of measuring hull speed.

Servo Control Module
The servo control module is used to output 4 PWM signals for our servo motor controls. The module uses two timer interrupts, one to set the PWM signal frequency of 50Hz and the other to set the duty cycle for each servo command. The current servo we are using, the TowerPro MG995, has a near 180° rotation range with corresponding duty cycle timing of ranging from 0.7 to 2.3 ms. The individual duty cycle times for each servo are cascaded every PWM period, allowing for multiple servo control using only the 2 timers. Figure 38 graphically depicts how the cascade works.

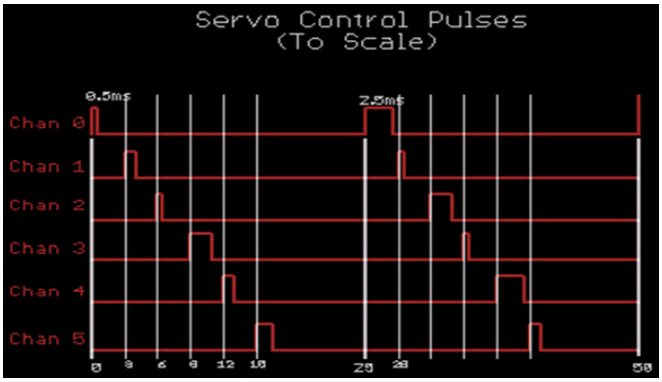

Figure 38: Multi servo pulse control

The precision of the pulse timer is down to a single µs, which allows us to precisely control the servo position. The MG995 is not an extremely accurate position tracker, but the fine tune ability of our control module allows us to slowly adjust the pulse widths to obtain a desired position. The module has to ways set the servo pulse width. One accepts the integer value of pulse length while the other accepts a degree value and converts the value to approximate pulse width for degree position. The purpose for the two inputs is to allow us to punch the servo position to a ball park of the desired orientation and then precisely increment to get exact position desired.

CAN Communication Module
Currently this module has not been created. This module will be used eventually as the user interface as is the client

specification. But for progress towards completing the wing control, the module is not imminently necessary.

IMU Module

Currently, this module is not complete. The MPU 6000 will be read through SPI and the Magnetometer is read through I2C. This module will be necessary when the controller design progresses to level of accounting for attitude of the wing.

II. System Controller

Currently the controller exists only on a conceptual level. The Controller has yet to be integrated into software.

IV. Future Steps

The currently completed coding modules and current hardware progress are nearly sufficient to allow us to begin designing and testing the previously described main inner loop of our controller. The only additional requirement is to skin the wing, which will be completed before courses officially reconvene. The internal control loop should remain nearly unchanged with or without the incorporation of attitude and vessel speed measurements. Additionally, testing the inner loop controller will allow us to experimentally determine the exact characteristics of the physical system, which is necessary information for implementing our controller design. In order to begin designing the entire controller, the GPS and IMU modules will need to be created, as they are necessary components of the moving vessel controller design. Once all necessary coding modules are complete, the project will enter the main testing and refining stage, which is the major aspect of the controls development for this project. If we are able to successfully validate the functionality of our control system with enough time left on the project, we will attempt to actually retrofit the wing onto a vessel and put the wing into actual test application.

V. Conclusion

The design and development of the Smart Wing has proven to be a challenge in all of its engineering aspects and a great test of the years of knowledge and experience that we have collected in our undergraduate endeavors. We have so far been able to deconstruct the many aspects of the Smart Wing into various design challenges and we have attempted to calculate, estimate, justify, and catalog all of our design choices throughout the process. So far we have accomplished a great deal of the mechanical design and construction of the Smart Wing. Since the beginning we have realized that this project is very dependent on the functionality and responsiveness of the wing mechanics and our persistence and meticulousness with the construction and design of the Smart Wing's mechanics and components have allowed us to produce a robust and responsive mechanical system. In turn the mechanical system would seem lacking without the great amount of electrical design we have completed to accompany the wing, its power supply, and sensing system, which includes robust signal conditioning circuitry and integration of efficient power conversion. Finally we have developed over the last quarter the critical programming modules that we will use to create our control system and bring the Smart Wing to life. These challenges have of course caused us to develop and redevelop designs through a healthy process of failure and redesign that have honed the current system into a more efficient and robust creation. We are looking forward to a final quarter which will hopefully conclude in successful testing of our design on an actual vessel.

Acknowledgment

We'd like to thank our senior design advisors, Patrick Mantey, and Jeff Bertalotto for their insight and guidance throughout this process. We would like to thank our advising professor Gabriel Elkaim for the chance to work on developing such an interesting system. Finally, we would like to thank UC Santa Cruz, Jack Saskin School of Engineering, and the BELS staff for providing the facilities and support necessary for this project.

References

[1] Elkaim, G.H., Gebre-Egziabher, D., Powell, J.D., Parkinson, W.B., *System Identification for Presicion Control of a Wingsailed GPS-Guided Catamaran*, 2001. P. 1-23.

[2] Shukla, P.C., Ghosh, K., *Revival of the Modern Wing Sails for thePropulsion of Commercial Ships*, 2009. P. 5-7.

[3] The OpenUniversity, *Are Cylinder ships a dead end invention?*, http://www.open.edu/openlearn/science-maths-technology/engineering-and-technology/design-and-innovation/invention-and-innovation-introduction/content-section-6.2

[4] Latham, J, Futuristic fleet of 'cloudseeders', http://www.webcitation.org/69QeZACfO

[5] Worsley, Peter. "Wingsailing." Wingsailing Experiments. N.p., n.d. Web. 25 Nov. 2014.

[6] Senga, H., Kato, N., Suzuki, H., Lubin, Y., Yoshie, M., *Toshinari TanakaField experiments and new design of a spilled oil tracking autonomous buoy*, 2013. P. 1-3.

[7] Sauz´e, C., Neal, M., *An Autonomous Sailing Robot for Ocean Observation*, 2006. P. 1

[8] Rodrigue, Dr. *Fuel Consumption by Containership Size and Speed*. N.p., n.d. Web. 10 Dec. 2014.